ACCURATE VIDEO-RATE MULTI-SPECTRAL IMAGING USING IMEC SNAPSHOT SENSORS

Kathleen Vunckx, Wouter Charle

imec vzw, Kapeldreef 75, 3001 Leuven, Belgium

ABSTRACT

Imec's pixel-level integration of spectral filters enables video-rate multi-spectral imaging with very compact cameras which are well-suited for precision agriculture and remote sensing. Current data processing techniques were limited to the reconstruction of spectral reflectance or transmittance and required the subsequent measurement of a spectrally uniform reference target covering the full field-of-view. In this paper, we present a new data processing flow to reconstruct both spectrally and spatially accurate spectral irradiance and reflectance, transmittance or exitance images even when only a small patch of a reference target is visible in only one of the acquired frames or when only a spectrometer measurement of the illumination spectrum is available. The accuracy is illustrated on lab and outdoor measurements. The presented data processing flow facilitates the use of the imec snapshot cameras for nearly any application, from disease detection in an orchard over coastal water quality inspection to accurate object tracking in spectral videos.

***Index Terms*—** video-rate, multi-spectral, snapshot, imaging, camera

1. INTRODUCTION

Traditionally, spectral imaging systems are implemented as wavelength or line scanning systems. This requires a time-multiplexed data acquisition, during which either the filter or scanning location is varied linearly to get a full three-dimensional spectral data cube. Many alternative acquisition systems exist conceptually to remove the time-multiplexing constraint and acquire three-dimensional spectral data in a snapshot fashion [1]. The most important benefit of a snapshot spectral system is that it acquires all data simultaneously and thus has the potential to cope with complex scenes with various motions as well as provide more freedom to integrate the imaging system in complex setups.

Imec has implemented a snapshot technology on chip, dividing the focal plane by repetition of a multispectral filter pattern [2], [3]. E.g., a 4x4 pattern divides the focal plane of 2048x1088 pixels in 16. Due to this spatial multiplexing, naively one would say that the spatial resolution of the sensor is reduced by the size of the pattern, but this resolution can partially be recovered, as will explained in this paper. As a result of the pixel level filter integration, this type of cameras also suffers more from cross talk than time-multiplexed systems. Hence, spectral correction is required to ensure accurate measurement of spectral irradiance, reflectance, transmittance or exitance.

This technology is available for spectral imaging in the VIS, Red-NIR and NIR range and integrated in different cameras from vendors like XIMEA, Photonfocus and others. Recently, imec also developed a snapshot SWIR camera.

In this article, we describe a new data processing flow, which is applicable both to these snapshot cameras and imec snapscan cameras [4], [5]. It will also be explained how it enables accurate spectral and spatial reconstruction of spectral irradiance and spectral reflectance, transmittance or exitance.

2. NEW DATA PROCESSING FLOW

To convert the raw measurements to spectral reflectance, transmittance or exitance, the following steps need to be followed:

- Dark level or bias correction (see section 2.1).
- Conversion from frame(s) to a set of aligned band images (one per filter). The different substeps, i.e. demosaicing, band alignment and spatial resampling are discussed in section 2.2.
- Conversion from a set of band images to a spectral irradiance cube, which entails spectral correction, angularity correction and non-uniformity correction as will be explained in section 2.3.
- Spectral normalization or white balancing (see section 2.4).

2.1. Dark level or bias correction

To correct for the dark level, an average dark measurement is acquired by covering the lens. The same integration time (and sensor temperature) should be used as for the scene measurement(s). This average dark frame is then subtracted from the scene frame.

2.2. Simultaneous band alignment & spatial upsampling

Like in RGB image sensors, the different spectral filters on an imec snapshot image sensor are repeated in an n-by-n mosaic pattern in which every filter covers a single pixel. When simply demosaicing the acquired images into separate band images, these band images are slightly misaligned with respect to each other. To align the images, we use the coordinate system of the original frame and transfer these coordinates to the band images. Next, bi-linear interpolation is used to resample the band images with a common grid, e.g. the grid of the original frame or a grid with a sample point in the center of every macro-pixel (i.e., n-by-n pixels).

2.3. Spectral irradiance

2.3.1. Spectral correction

In [6], a method to spectrally correct reflectance corrected data was described. It was shown that one can compute a simple 2D correction matrix for this.

Here, we adjust this method to enable spectral correction of raw, dark corrected data. The linear combination of measured filter or band responses B is sought which approximates best – in least square sense – the fitted normalized ideal band responses B^{ideal}. In other words, a matrix C – called the radiometric or irradiance correction matrix – is computed which minimizes the Frobenius norm of the error between B^{ideal} and its approximation:

$$\arg\min_{C} \left\| B^{ideal} - BC \right\|_F$$

By applying the correction matrix C to the raw, dark corrected stack of band images and due to the normalization of the ideal filter responses, we can predict what an ideal multi-spectral camera would measure, i.e. if the camera would have a spectral resolution defined by the full-width-at-half-maximum of the fitted ideal Fabry-Pérot responses and would not suffer from cross talk.

2.3.2. Angularity correction

In [7], it is explained how the transmission response of interference based filters like the ones integrated in the imec snapshot sensors changes with the angle of incidence of the light and how this can be corrected for when one knows the f-number of the lens and the distance between the exit pupil of the lens and the image sensor. Details about the angularity correction method can be found in [7].

2.3.3. Non-uniformity correction

The pixel response of a CMOS imager can vary slightly across the sensor. Furthermore, the lens can also cause a spatially variant pixel response due to vignetting. These effects can be compensated for by dividing the reconstructed cube point-by-point by a non-uniformity correction cube.

The computation of a non-uniformity correction cube requires an extra calibration measurement once to be performed in the lab with the full system as (it will be) used later, i.e. with the same lens and f-number. The measurement can be done using either an integrating sphere or a white reflectance tile as illustrated in Figure 1. The irradiance spectrum of the illumination should be known. An average dark measurement is also needed for dark level correction (see section 2.1). The same calibration setup can be used for snapshot and snapscan cameras.

When you use a white reflectance tile, the intensity of the illumination will usually not be fully homogeneous. The spatial non-uniformity of the illumination then needs to be estimated and divided away. This can be done after the frame has been dark level corrected and converted to aligned and resampled band images (see sections 2.1 and 2.2). Next, the set of band images need to be spectrally and angularity corrected as explained in sections 2.3.1 and 2.3.2. The processing steps should be identical to those which will be applied to the scene frames later.

At this point, the reconstructed irradiance of the calibration measurement still contains the irradiance spectrum of the illumination used during calibration. This should be divided away to yield the non-uniformity correction cube. Note that the resolution of the spectrometer measurement of the illumination spectrum needs to be matched to that of the spectral camera prior to the division to avoid artifacts in the reconstructed spectrum. Furthermore, the spectrometer measurement should be converted to photon counts and properly scaled.

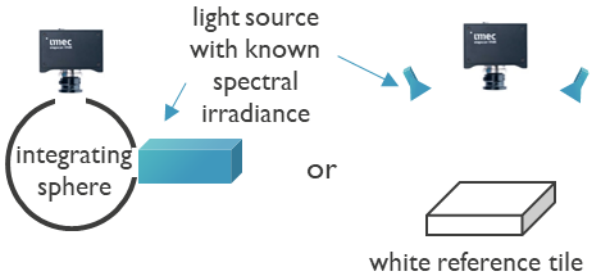

Figure 1: Two alternative measurement setups for obtaining the non-uniformity correction cube.

2.4. Spectral reflectance, transmittance or exitance

The reconstructed spectral irradiance of the scene also still contains the irradiance spectrum of the illuminant. If a white or gray reference target (which reflects the same fraction of the incident light for every wavelength in the range of interest) is present in the scene, its reconstructed spectral irradiance should be identical (up to a scale factor) to the

measured spectral irradiance of the light source (expressed in photons/s/nm) with an ideal multi-spectral camera.

To cancel out the spectral irradiance of the illumination, one can divide the reconstructed spectral irradiance in every pixel by the (average) reconstructed spectral irradiance in one or more pixels of the white or gray reference tile and multiply by the spectral reflectance value of the tile, e.g. 0.95 or 0.5. As long as the illumination is stable, it is sufficient that the reference tile is visible in part of one of the scenes.

As an alternative, any other reference point or region in the scene can be used for spectral normalization or white balancing, as long as the reflectance spectrum (or transmittance or exitance spectrum in case of transmittance or exitance imaging) is known and sufficiently high for all wavelengths to limit the loss in signal-to-noise ratio.

Since the data were converted to spectral irradiance, one can also simply divide away the spectral irradiance of the illumination measured with a calibrated point spectrometer. As explained in section 2.3.3, the spectral resolution of the spectrometer should be matched to the resolution of the snapshot camera to avoid spectral artifacts. If the position of the spectrometer is fixed with respect to the position of the spectral camera, a scaling factor will need to be determined only once using a reference reflectance target.

3. EXPERIMENTS

3.1. RedNIR measurement of a resolution target

To investigate the impact of band alignment and spatial upsampling on the spatial and spectral quality of the reconstructed multi-spectral cube, a black and white resolution chart was measured in the lab under halogen illumination using a XIMEA snapshot RedNIR camera.

3.2. Outdoor spectral reflectance measurements (VIS)

To illustrate that it is sufficient to have a small white reference tile which is only visible in one scene to obtain accurate reflectance spectra in all scenes, a set of images of different scenes with and without spectral reference targets was taken outdoor in a time span of 20 minutes with a XIMEA snapshot VIS camera.

3.3. Outdoor spectral exitance measurements (VIS)

The same XIMEA snapshot VIS camera was also used to acquire a video of a large crossing with many traffic lights. A white arrow on one of the road signs in one of the frames was used for white balancing in this case.

4. RESULTS

4.1. Impact band alignment & spatial upsampling

A zoom-in on a part of the reconstructed resolution chart is shown in Figure 2. Each subimage corresponds to the reflectance image at a specific wavelength. At the top, the result of band alignment without upsampling is shown. At the bottom, the result of band alignment with upsampling is shown.

To further illustrate the improvement in spatial resolution, a profile is plotted through the different parallel lines in the 9th wavelength image in Figure 3. A clear increase in constrast is observed in the upsampled images (see Fig. 2 & 3, (b) vs. (a)).

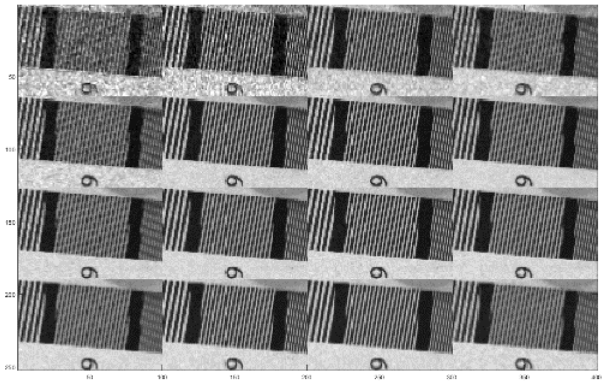

(a)

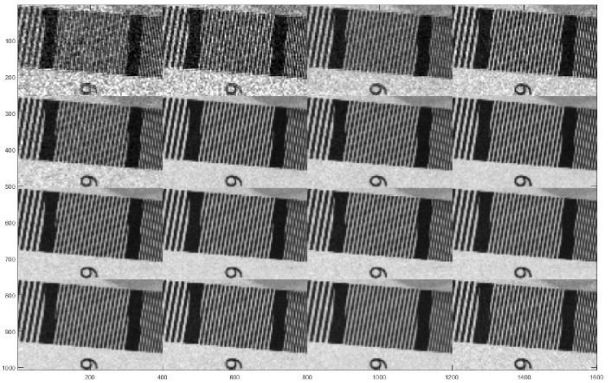

(b)

Figure 2: Reconstructed reflectance images. Different tiles represent different wavelengths. (a) Band alignment and no upsampling, (b) band alignment and 4x upsampling.

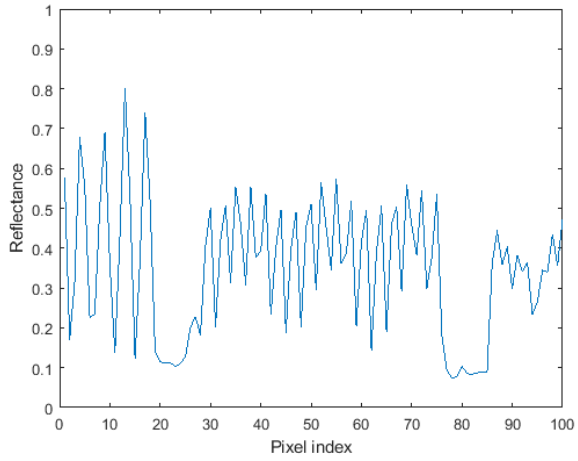

(a)

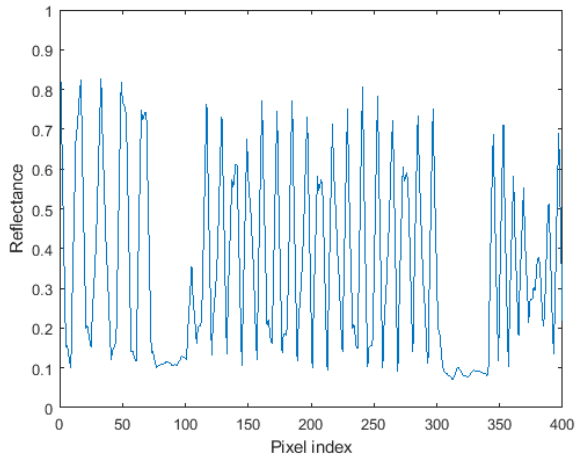

(b)

Figure 3: Profile through the different parallel lines in the 9th wavelength image. (a) Through row 150 in Figure 2(a), (b) through row 600 in Figure 2 (b).

4.2. Spectral irradiance accuracy

To investigate the accuracy of the reconstructed spectral irradiance, the processing of the measurement is stopped after non-uniformity correction, but before white balancing. This was done with band alignment, both with and without spatial upsampling (see section 2.2).

In Figure 4, the average reconstructed irradiance spectrum in a small region-of-interest in a white area of the resolution chart is plotted on top of a point spectrometer measurement of the halogen spectral irradiance (in photon counts, arbitrary scaling). As can be seen, both reconstructed spectral irradiance curves closely match the spectrometer measurement.

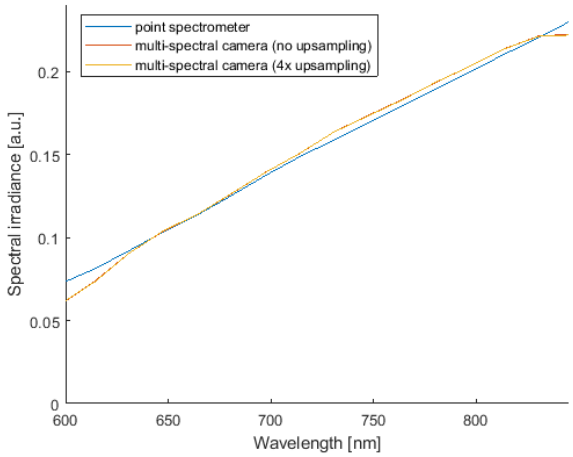

Figure 4: Reconstructed spectral irradiance spectrum of the halogen illumination measured in a small region-of-interest in a white area of the resolution chart compared to a point spectrometer measurement.

4.3. Spectral reflectance accuracy

One of the outdoor scenes contained a white reference tile (see Figure 5(a)), which was used for spectral normalization or white balancing (see section 2.4). In another scene, no spectral targets were present (see Figure 5(b)). In the other scenes a Datacolor SpyderCHECKR was positioned at different locations in the field-of-view. The RGB images shown in Figure 5 are computed from the multi-spectral data.

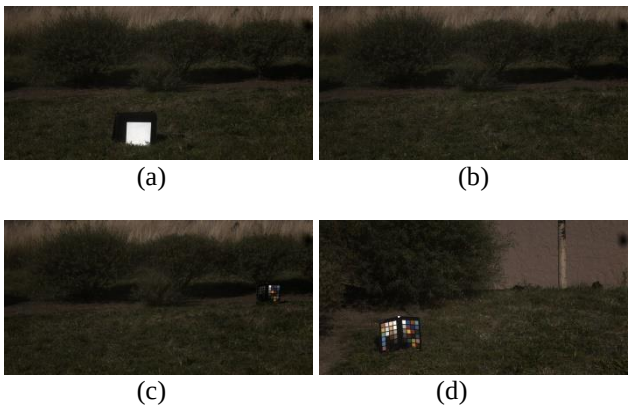

(a) (b)

(c) (d)

Figure 5: Reconstructed RGB images of the different scenes with/without spectral reference targets at different locations in the field-of-view.

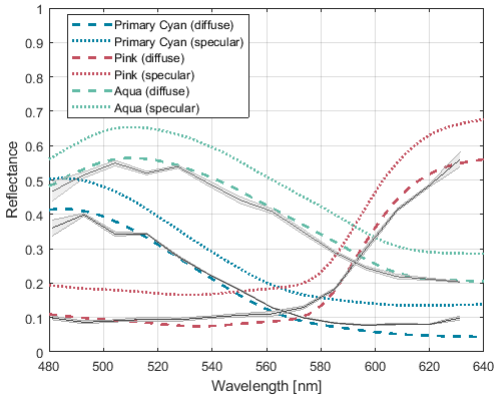

(a)

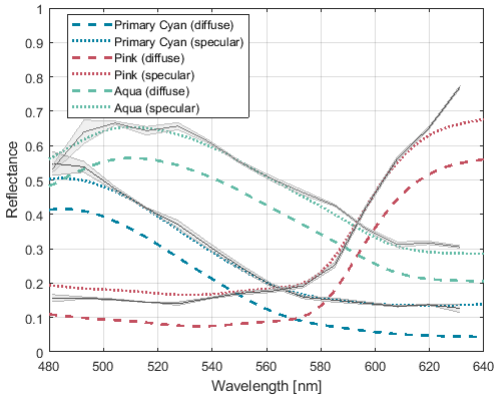

(b)

Figure 6: Reconstructed reflectance spectra (gray) plotted together with the diffuse and specular reflectance measurement obtained with a point spectrometer. (a) Spectra from 3 reference tiles in Figure 5(c). (b) Spectra from the same reference tiles in Figure 5(d).

In the plots in Figure 6, you can see the diffuse (dashed lines) and specular (dotted lines) reflectance spectrum of 3 tiles of the color chart measured with a point spectrometer. In gray, you see the snapshot measurement of these tiles when they were positioned at different locations in the field-of-view. The spectra from the measured scenes shown in Figure 5(c) and 5(d) are plotted in Figure 6(a) and 6(b), respectively. Depending on the orientation of the chart with respect to the sun, the reflectance spectrum matches more closely to the diffuse or to the specular measurement.

4.4 Spectral exitance measurements

Each frame of the multi-spectral video was processed with the newly proposed data processing flow (see section 2). For the white balancing step, the reconstructed reflectance spectrum of a point in the white arrow on the road sign in the middle of the crossing was used.

Furthermore, an RGB image was also computed from each frame, to mimic an acquisition with an RGB camera. For that, a correction matrix was used which approximates best the typical RGB band responses by a linear combination of measured bands. An example RGB frame is shown in Figure 7. A zoom-in on the RGB reconstruction of the 5 traffic lights facing the camera can be found in Figure 8(a) and nicely illustrates that red and orange can fairly easily be mistaken when judging purely based on color in an RGB image or on RGB values (see Figure 8(b) top plots). However, when looking at the spectral exitance spectrum reconstructed from a multi-spectral frame (see Figure 8(b) bottom plots), red and orange can easily be distinguished.

Figure 7: RGB image of a large crossing with 5 traffic lights.

(a)

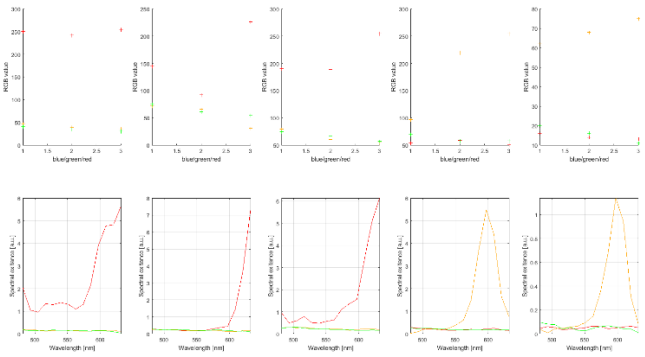

(b)

Figure 8: (a) Zoom-in on the 5 traffic lights facing the camera, extracted from the reconstructed RGB image. (b) Reconstructed RGB (top) and spectral exitance values (bottom) for the 5 traffic lights in that scene.

5. DISCUSSION

Accurate spectral reconstruction is important for many different use cases:

- Comparison to a database of known spectra.
- Quantitative analysis (to determine the composition of a material).
- Follow up of a spectral signature over time (seconds, hours, days, months, ...).
- Reproducibility of measurement data.
- Combination of data from multiple cameras of the same or different spectral ranges.
- ...

The new data processing pipeline facilitates the use of all multi- and hyperspectral cameras with imec's pixel level integrated spectral filters for applications where the light conditions can be varying and a full field-of-view spectral reference scan is not possible, e.g. environment monitoring.

Since snapshot spectral cameras are quite unique in video-rate spectral imaging, this opens the door for an even broader spectrum of applications, like disease inspection of an orchard by mounting a camera on a tractor or on a UAV, python detection [8] or surveillance. As an example, it was recently shown that object tracking is more robust when applied on multi-spectral data from a XIMEA snapshot VIS camera than on standard RGB data [9]. To further boost the development of object tracking algorithms for multi- and hyperspectral imaging, the same camera has been used to generate a large training and test data set of multi-spectral videos for a hyperspectral object tracking challenge, organized in conjunction with Whispers 2021 [10].

Integrating a point spectrometer with a spectral camera in one system can be useful for systems which need to be operated under rapidly changing light conditions, e.g. outside imaging from a drone or a tractor on a day with scattered clouds. An additional absolute calibration of the spectral camera with respect to the spectrometer should then also be required once (for a fixed lens and f-number), like it is also the case for the calibration scan to determine the non-uniformity correction (see section 2.3.3). If the lens which is used has significant vignetting, it is recommended to use an integrating sphere to obtain the non-uniformity correction cube, such that the fall-off due the vignetting is not divided away when removing the estimated light fall-off pattern and therefore will cancel out when applying non-uniformity correction.

6. CONCLUSION

In this paper, it is shown that both spectrally and spatially accurate spectral irradiance and reflectance, transmittance or exitance images can be reconstructed from video-rate spectral cameras with imec's snapshot sensors. The new data processing flow enabling this is presented and the accuracy is illustrated based on both lab and outdoor measurements.

The spatial resolution can be improved by band alignment and spatial upsampling, while the spectral accuracy benefits from applying spectral correction directly to the dark corrected, band aligned images. Further improvements in spectral quality are achieved by performing angularity and non-uniformity correction.

The two main novelties of this new method are that it enables the reconstruction of spectral irradiance images and the reconstruction of spectral reflectance, transmittance or exitance images, even when only a small patch of a reference target is visible in only one of the acquired snapshot frames or when only a spectrometer measurement of the illumination spectrum is available.

As a result, video-rate spectral cameras with imec snapshot sensors can be used for nearly any application, from disease detection in an orchard over coastal water quality inspection to accurate object tracking in spectral videos.

7. ACKNOWLEDGEMENTS

The authors would like to thank their colleagues from the Integrated Imaging team at imec, Caglar Kalaycioglu and Carolina Blanch for the help with the acquisition of the data sets and Vincent Radelet for the implementation of the new data processing pipeline in HSI Mosaic.

8. REFERENCES

[1] N. Hagen, R. T. Kester, L. Gao, and T. S. Tkaczyk, "Snapshot advantage: a review of the light collection improvement for parallel high-dimensional measurement systems," *Opt. Eng*., 51(11):111702, 2012. https://doi.org/10.1117/1.OE.51.11.111702

[2] N. Tack, A. Lambrechts, P. Soussan, and L. Haspeslagh, "A compact, high-speed, and low-cost hyper-spectral imager," *Proc. of SPIE*, Vol. 8266, Silicon Photonics VII, 82660Q, 2012. https://doi.org/10.1117/12.908172

[3] B. Geelen, N. Tack, and A. Lambrechts, "A compact snapshot multispectral imager with a monolithically integrated per-pixel filter mosaic," *Proc. of SPIE*, Vol. 8974, Advanced Fabrication Technologies for Micro/Nano Optics and Photonics VII, 89740L, 2014. https://doi.org/10.1117/12.2037607

[4] J. Pichette, W. Charle, A. Lambrechts. "Fast and compact internal scanning CMOS-based hyperspectral camera: the Snapscan", *Proc. of SPIE*, Vol. 10110, Photonic Instrumentation Engineering IV, 1011014, 2017. https://doi.org/10.1117/12.2253614

[5] P. Gonzalez, J. Pichette, B. Vereecke, B. Masschelein, L. Krasovitski, L. Bikov, A. Lambrechts, "An extremely compact and high-speed line-scan hyperspectral imager covering the SWIR range," *Proc. of SPIE*, Vol. 10656, Image Sensing Technologies: Materials, Devices, Systems, and Applications V, 106560L, 2018. https://doi.org/10.1117/12.2304918

[6] J. Pichette, T. Goossens, K. Vunckx, and A. Lambrechts, “Hyperspectral Calibration Method For CMOS-based Hyperspectral Sensors,” *Proc. of SPIE*, Vol. 10110, Photonic Instrumentation Engineering IV, 101100H, 2017. https://doi.org/10.1117/12.2253617
[7] T. Goossens, K. Vunckx, A. Lambrechts, and C. Van Hoof, “Spectral Shift Correction for Fabry-Perot Based Spectral Cameras”, *10th Workshop on Hyperspectral Imaging and Signal Processing: Evolution in Remote Sensing (WHISPERS)*, Amsterdam, The Netherlands, 24-26 Sept. 2019. https://doi.org/10.1109/WHISPERS.2019.8920890
[8] R. Driggers, O. Furxhi, G. Vaca, V. Reumers, M. Vazimali, R. Short, P. Agrawal, A. Lambrechts, W. Charle, K. Vunckx, and C. Arvidson, “Burmese python target reflectivity compared to natural Florida foliage background reflectivity,” *Applied Optics*, Vol. 58, No. 13, pp. D98-D104, 2019. https://doi.org/10.1364/AO.58.000D98
[9] F. Xiong, J. Zhou, and Y. Qian, “Material based object tracking in hyperspectral videos,” IEEE Trans. Image Process., Vol. 29, No. 1, pp. 3719-3733, 2020.
[10] J. Zhou, P. Ghamisi, F. Xiong, J. Chanussot, “Hyperspectral object tracking challenge”, https://www.hsitracking.com/, Amsterdam, The Netherlands, 14-16 Jan. 2021.